

Supplementary Materials

# Influence of Dispersion and Orientation on Polyamide-6 Cellulose Nanocomposites Manufactured through Liquid-Assisted Extrusion

Luísa Rosenstock Völtz <sup>1,2</sup>, Shiyu Geng <sup>1,2</sup>, Anita Teleman <sup>3</sup> and Kristiina Oksman <sup>1,2,4,\*</sup>

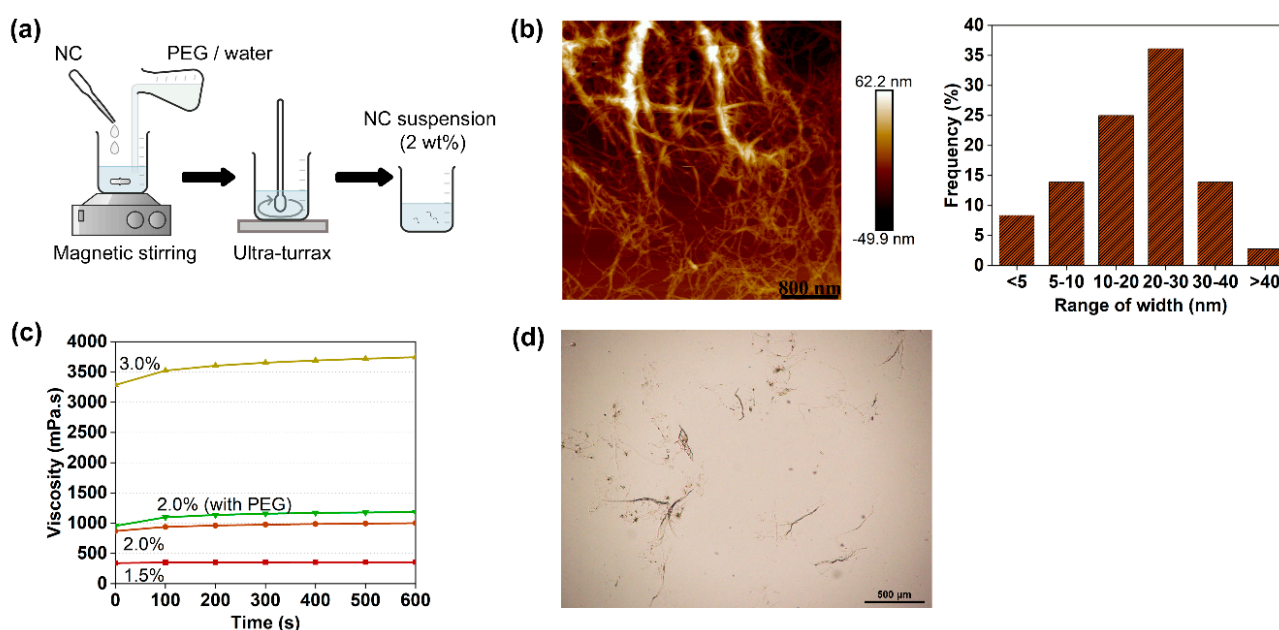
<sup>1</sup> Division of Materials Science, Department of Engineering Sciences and Mathematics, Luleå University of Technology, SE-97187 Luleå, Sweden; luisa.voltz@ltu.se (L.R.V.); shiyu.geng@ltu.se (S.G.)

<sup>2</sup> Wallenberg Wood Science Center (WWSC), Luleå University of Technology, SE-97187 Luleå, Sweden

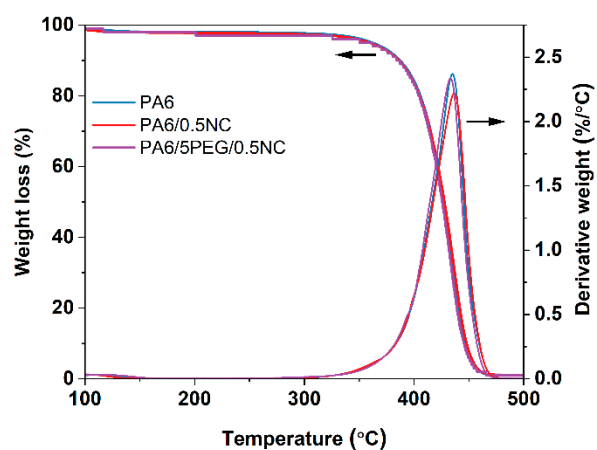
<sup>3</sup> RISE Research Institutes of Sweden, SE-11486 Stockholm, Sweden; anita.teleman@ri.se

<sup>4</sup> Department of Mechanical & Industrial Engineering (MIE), University of Toronto, Toronto, ON M5S 3G8, Canada

\* Correspondence: kristiina.oksman@ltu.se



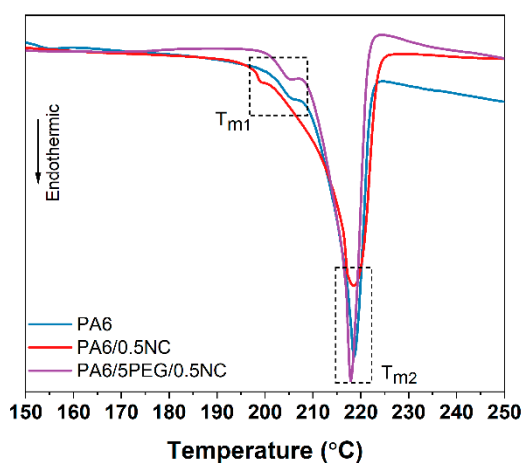
**Figure S1.** (a) NC suspension preparation by adding water and/or PEG following by magnetic stirring and ultra turrax; (b) AFM micrograph of the nanocellulose (0.01 wt.%) and width distribution of the nanocellulose; (c) viscosity versus time curves for different NC concentrations (1.5, 2 and 3 wt.% water base and 2 wt.% PEG/water base) and (d) OM image of NC suspension (0.01 wt.%), scale bar 500 μm



**Figure S2.** Thermogravimetric curves for PA6 and PA6-nanocomposites measured by TGA. The onset degradation temperature for PA6: 403 °C, PA6/0.5NC: 402 °C, and PA6/5PEG/0.5NC: 402 °C

**Table S1.** Degree of crystallinity ( $X_c$ ) and melting peaks measured by DSC. The samples were dried prior testing.

Sample	$X_c$ (%)	$T_{m1}$ (°C)	$T_{m2}$ (°C)
PA6	21	205	218
PA6/0.5NC	28	200	218
PA6/5PEG/0.5NC	25	205	218
OPA6	31	210	221
OPA6/0.5NC	42	212	222
OPA6/5PEG/0.5NC	30	210	221

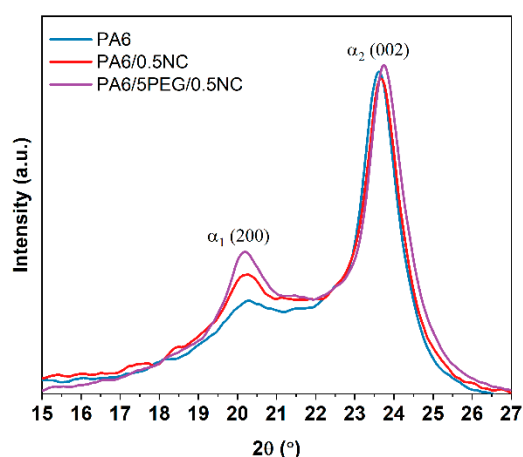
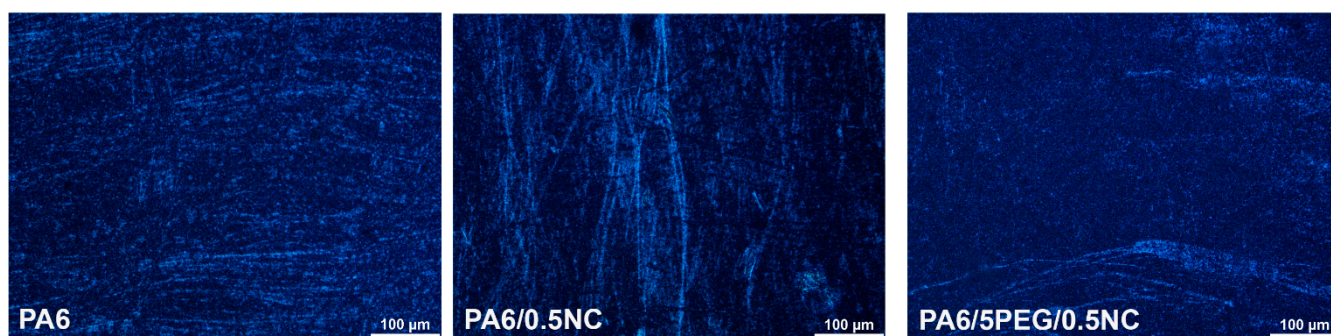


**Figure S3.** DSC curves for PA6 and PA6-nanocomposite. The double melting peaks,  $T_{m1}$  and  $T_{m2}$ , are shown in the graph

**Table S2.** Tensile properties of non-oriented PA6 and PA6-nanocomposites. The toughness was calculated by the area under the stress-strain curve

Sample	Strength (MPa)	Modulus (GPa)	Elongation at break (%)	Toughness (MJ/m <sup>3</sup> )
PA6	61 ± 2 <sup>A</sup>	2.0 ± 0.1 <sup>A</sup>	21 ± 8 <sup>A</sup>	11.5 ± 4.4 <sup>A</sup>
PA6/0.5NC	60 ± 1 <sup>A</sup>	2.3 ± 0.1 <sup>B</sup>	19 ± 6 <sup>A</sup>	10.4 ± 2.9 <sup>A</sup>
PA6/5PEG/0.5NC	52 ± 1 <sup>B</sup>	1.4 ± 0.1 <sup>C</sup>	63 ± 4 <sup>B</sup>	29.5 ± 2.5 <sup>B</sup>

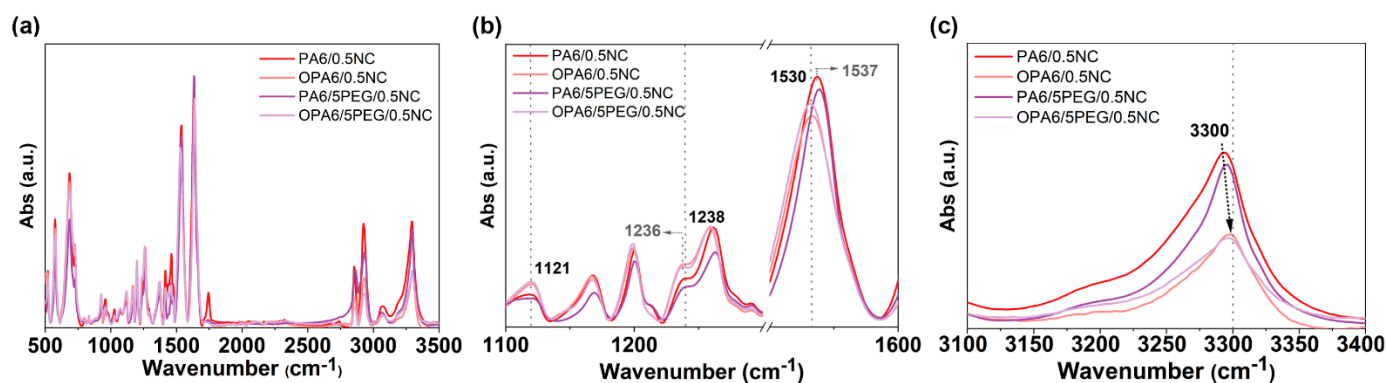
<sup>A,B,C</sup> Marked with the same letter within the same column are not significantly different at a 5% significance level based on ANOVA and Tukey's Test.

**Figure S4.** 1D-XRD for PA6 and PA6-nanocomposite. The first peak around 20.2° is related to  $\alpha_1$  crystals (200) and the second peak around 23.7° to  $\alpha_2$  crystals (002)**Figure S5.** POM using hot-stage (220 °C) for PA6 and PA6-nanocomposites at 90 seconds (scale bar 100 μm).

**Table S3.** Tensile properties of oriented PA6 and PA6-nanocomposites. The toughness was calculated by the area under the stress-strain curve

Sample	Strength (MPa)	Modulus (GPa)	Elongation at break (%)	Toughness (MJ/m <sup>3</sup> )
OPA6	203 ± 5 <sup>A</sup>	2.6 ± 0.1 <sup>A</sup>	24 ± 4 <sup>A</sup>	34.0 ± 7.6 <sup>A</sup>
OPA6/0.5NC	215 ± 7 <sup>B</sup>	3.0 ± 0.2 <sup>B</sup>	18 ± 3 <sup>B</sup>	24.3 ± 6.2 <sup>B</sup>
OPA6/5PEG/0.5NC	221 ± 5 <sup>B</sup>	2.8 ± 0.2 <sup>A/B</sup>	23 ± 1 <sup>A</sup>	33.6 ± 3.4 <sup>A/B</sup>

<sup>A,B,C</sup> Marked with the same letter within the same column are not significantly different at a 5% significance level based on ANOVA and Tukey's Test.

**Figure S6.** FT-IR spectra for PA6-nanocomposites and OPA6-nanocomposites, (a) FTIR spectra from 500 to 3500 cm<sup>-1</sup>; (b) from 1100 to 1600 cm<sup>-1</sup>; and (c) from 3100 to 3400 cm<sup>-1</sup>.**Table S4.** Apparent crystallite size and diffraction angles measured by 1D-XRD scattering patterns

Sample	Crystallite size (nm)	2θ <sub>1</sub> (°)	2θ <sub>2</sub> (°)
PA6	5.32	20.3	23.6
PA6/0.5NC	7.79	20.2	23.7
PA6/5PEG/0.5NC	6.70	20.2	23.8
OPA6	3.88	20.6	23.2
OPA6/0.5NC	4.50	20.5	23.1
OPA6/5PEG/0.5NC	2.64	20.5	23.3

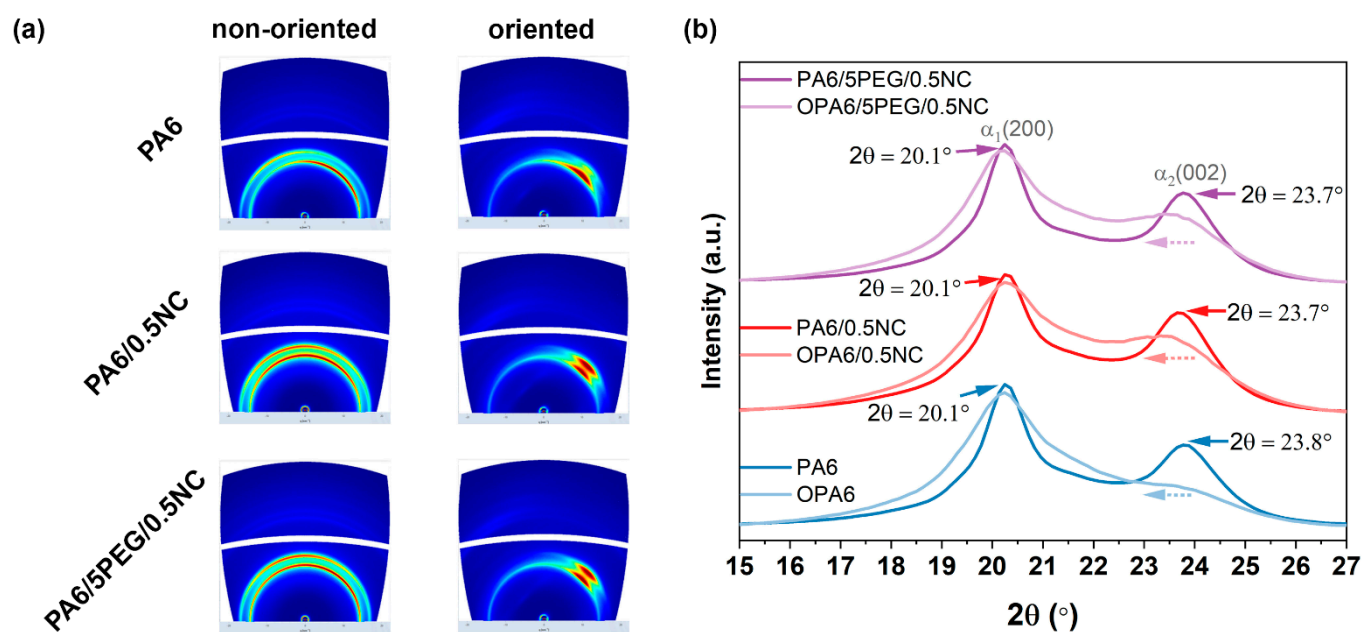


**Figure S7.** (a) 2D-WAXS diffractograms and (b) 2D-XRD scattering pattern for PA6 and PA6-nanocomposites before and after SSD

**Table S5.** Orientation index for crystalline PA6 in the composites, as estimated from WAXS measurements. If all crystalline PA6 is aligned in the same direction,  $f_c = 1$ , and if it is randomly distributed,  $f_c = 0$

Sample	Orientation index, $f_c$ <sup>1</sup>	
	Non-oriented	Oriented
PA6	0.60; 0.53	0.82; 0.83
PA6/0.5NC	0.32; 0.37	0.84; 0.84
PA6/5PEG/0.5NC	0.39; 0.42	0.86; 0.85

<sup>1</sup> Azimuthal integration of the  $\gamma(001)(200)$ ,  $\alpha(200)$  and  $\alpha(002)$  scattering planes,  $2\theta = 20.1 \pm 0.4^\circ$ ;  $23.7 \pm 0.4^\circ$ .